

Chlorine monoxide in the Antarctic spring vortex

1. Evolution of midday vertical profiles over McMurdo Station, 1993

R. L. de Zafra,¹ J. M. Reeves,² and D. T. Shindell

Physics Department, State University of New York, Stony Brook

Abstract. We have obtained a prolonged record of emission spectra from chlorine monoxide in the vicinity of McMurdo Station, Antarctica, during formation of the austral spring ozone hole of 1993. These spectra have been processed to obtain vertical mixing ratio profiles by deconvolution of pressure-broadened line shapes. The resulting profiles give a detailed evolution for both altitude distribution and mixing ratio of ClO during development of a major ozone hole event. In early September, very strong emission was observed from pressure-broadened low-altitude ClO. Deconvolutions show that this came from an unusually thick layer, extending well above 20 km in altitude. This layer decreased steadily in thickness through September, accompanied by a shift of the peak mixing ratio from ~21 km altitude in early September to ~17–18 km by the end of the month, indicating an apparent descent rate of order 100 meters per day, although we argue that the true descent rate is probably lower than the apparent rate. A brief, significant decrease in ClO content occurred in late September when the inner vortex edge (defined by the magnitude of Ertel's potential vorticity = $5.2 \cdot 10^{-5}$ at ~19–20 km) approached McMurdo, signifying that a strong gradient in ClO exists near the inner vortex edge. A rapid and apparently final deactivation of chlorine in the lower stratosphere was observed to start about October 1–2. The findings of initially large values of ClO well above 20 km are consistent with observation of polar stratospheric cloud formation in this range during the austral winter of 1993, and with observations showing increased ozone depletion above 20 km relative to previous years.

1. Introduction

The essential role of chlorine chemistry in causing massive annual spring ozone depletion over Antarctica has been clearly demonstrated through field measurements beginning in 1986 [de Zafra *et al.*, 1987; Solomon *et al.*, 1987; Brune *et al.*, 1989; de Zafra *et al.*, 1989], and a good theoretical understanding of the process has been established [e.g., Solomon, 1990]. The primary signature for chlorine chemistry is the formation of an anomalous layer of chlorine monoxide several kilometers thick in the lower stratosphere during the active period of ozone depletion. This low-altitude ClO begins a rapid buildup as soon as sunlight returns after the polar winter, although recent satellite mapping has shown that enhanced low-altitude ClO also can form in sunlit regions late in the Antarctic fall, if preceded by temperatures cold enough to cause formation of polar stratospheric clouds (PSCs) [Waters *et al.*, 1993]. PSCs provide the means, through rapid heterogeneous chemical processing on particle surfaces, to remove NO_x (largely through conversion to HNO_3), and thus prevent the sequestering of ClO in ClONO_2 . On occasion, volcanic aerosols may substitute for, or add to, the role played by PSCs, (now rather well established following the eruption of Mt. Pinatubo in 1991).

The Microwave Limb Sounder (MLS) on board NASA's Upper Atmosphere Research Satellite (UARS) has been producing large-area maps of ClO, derived from millimeter-wave emission spectroscopy, to a latitude limit of 80°S since September 1991 [e.g., Waters *et al.*, 1993]. Although this has allowed a revealing view of the seasonal buildup and areal extent of the anomalous low-altitude layer of chlorine monoxide, two factors arising from UARS orbital behavior impose significant limits on MLS seasonal and diurnal observations. First, the satellite is reversed in orientation approximately every 36 days, whereupon the southward limit of observation changes from ~-80° to -34°, well north of the region of ozone depletion. One of these northward reorientations occurs each year shortly after the middle of September, before completion of the ozone hole's formative phase, and before the final deactivation of chlorine within the vortex core can be detected. Second, the time of day during which measurements occur within a limited geographical region changes very slowly, so that coverage of a full diurnal cycle takes several weeks, during which photochemistry as well as temperature and transport within the vortex region produce substantial changes in ClO, independently of the diurnal cycle. The MLS is thus well suited for the important task of large-scale mapping of ClO but not as well suited for following secular evolution through a key period over Antarctica, or for detailing diurnal cycles.

We address these problems by presenting, in this paper, details of the secular change of ClO over McMurdo Station (77.9°S, 166.6°E) throughout most of the month of September and into October. In a companion paper [D. T. Shindell and R. L. de Zafra, Chlorine monoxide in the Antarctic spring vortex, 2: A comparison of measured and modeled diurnal cycling over

¹Also at Institute for Terrestrial and Planetary Atmospheres, State University of New York, Stony Brook.

²Now at Department of Atmospheric, Oceanic and Space Sciences, University of Michigan, Ann Arbor.

McMurdo Station, 1993, submitted to *J. Geophys. Res.*, 1994] we present data on the diurnal cycling of CIO and analyze this as a function of altitude, time-varying solar flux, and ambient temperature, all of which test current understanding of the catalytic chemistry of the CIO dimer and CIO-BrO cycles.

During September and October 1993, particularly favorable weather and positioning of the vortex made it possible for us to make a sustained series of observations showing much of the secular evolution of the low-altitude CIO layer during the period of most active ozone destruction. At the latitude of McMurdo ($\sim 78^\circ\text{S}$) the circumpolar transit time of air entrained in the vortex is about a week, so that although our observations are confined to a fixed ground location, in fact they sample a significant fraction of vortex air during the course of several days.

Ozone depletion was particularly severe in degree and geographical extent in the austral springs of both 1992 and 1993, reaching a low of <100 Dobson units (D.U.; $1 \text{ D.U.} = 2.69 \cdot 10^{16} \text{ molecules/cm}^2$) in column density in 1993 [e.g., Hofmann *et al.*, 1994; Johnson *et al.*, 1995]. It is assumed that the increased aerosol loading of the stratosphere following the explosion of Mt. Pinatubo in June 1991 was responsible for the severity of depletion in 1992, in large part due to the rapidity and thoroughness of lower stratospheric denitrification by heterogeneous chemical processing on the additional sulfuric aerosol. The special circumstances marking 1993 are less obvious, since Pinatubo aerosols no longer contributed significantly to the surface loading above $\sim 16 \text{ km}$, and provided 20–25% less surface loading in the 11–16 km range than in 1992 [Johnson *et al.*, 1995]. We will explore some possible factors after describing the data collected in 1993.

2. Instrumentation and Observing Technique

Beginning with our 1992 Antarctic observations [Emmons *et al.* 1995], we have used a new, high-sensitivity mm-wave receiver, and in 1993 added a new acousto-optical spectrometer with a slightly wider spectral band pass (600 MHz) and a resolution of 2 MHz. The mm-wave receiver consists of a superconducting tunnel-junction heterodyne mixer [de Zafra *et al.*, 1994] operated at 4.5 K by a closed-cycle helium refrigerator. Sky signals are passed through a sideband filter to suppress the image sideband and yield single-sideband spectra.

The overall system noise temperature is typically $\leq 350 \text{ K}$ (including receiver losses, mixer and IF amplifier noise), about a factor of 2 better than the previous Stony Brook mm-wave spectrometer, allowing integration times to be shortened by nearly a factor of 4 to achieve the same signal/noise ratio. With the present system, data averaged over a 1-hour time period, under the best observing conditions, give a high enough S/N ratio for reliable profile recovery. For conditions more typical at McMurdo, better results are obtained by combining data for the same time bins over 2 or 3 successive days, as is done for the data presented here. The general mode of observation is the same as that developed for our earlier system and described by Parrish *et al.* [1988].

3. Data Processing

We express spectral intensity in degrees Kelvin, taking advantage of the Rayleigh-Jeans blackbody radiation limit, which is appropriate with negligible error for the frequency and temperature range in question. This yields a conveniently linear relation between spectral intensity and temperature. Details of

the methods used to determine instrument sensitivity and to continuously monitor the tropospheric opacity (also necessary for a proper calibration of received signal intensity) are contained in Parrish *et al.* [1988] and de Zafra [1995]. As in our previous work, all measured spectral intensities are normalized to represent what would be seen in the zenith direction, in the absence of tropospheric attenuation. Self-absorption or attenuation by stratospheric background gases is negligible for CIO.

Overall calibration uncertainty from all contributions is estimated to be $\leq 8\%$ for the present system. This essentially altitude independent uncertainty must be added in quadrature to the altitude-dependent uncertainties arising from the deconvolution process and from uncertainties in input parameters, such as pressure and temperature profiles. This is discussed in further detail in an appendix to this article, and a summary of uncertainties is given in Table 1 for the peak of the anomalous low-altitude layer.

The spectral contributions from nearby ozone lines must be removed before the CIO emission lineshape can be deconvolved to retrieve a mixing ratio profile from its pressure-broadened line shape. We use day-minus-night differencing to do this [e.g., Emmons *et al.*, 1995], which takes advantage of the relative stability of ozone in the stratosphere over periods of a day or two versus the strong diurnal cycle exhibited by the anomalous low altitude CIO layer under study here.

In practice, the receiver/spectrometer is run 24 hours a day, weather permitting. Predawn spectra, covering a period up to 4 hours before sunrise (or within 2 hours before sunrise when the night period becomes short after the end of September), contain a minimal remaining CIO signal from low altitudes, due to the rapid recombination of CIO into its dimer form when photolysis stops. The remaining narrow signal from high-altitude CIO above $\sim 30 \text{ km}$ (only about 20% of the total spectral band pass) is "blanked out" of the spectrum, and a second-order background curve to fill the resulting gap is fitted to the ozone line shape on each side of the blanked portion. In addition to the ozone emission spectrum, this "blanked and filled" spectrum still contains any artifacts induced by the apparatus (for instance, remnant standing-wave undulations), and to the extent that these remain relatively stable over 12- to 24-hour periods, subtracting this prepared nighttime spectrum from daytime spectra will remove both the ozone line and the spectral artifacts. Generally this procedure works very well, and virtually no trace of the ozone emission line survives in the differenced spectra. Baseline artifacts are also generally reduced to a small fraction of the CIO signal amplitude.

This subtraction method will yield a true representation of the midday low-altitude layer only if spectral emission from this layer has diminished to negligible intensity by the predawn hours. The experimental data (e.g., see paper 2) show that a rapid decrease from midday values begins significantly before

Table 1. Error Budget for Retrieved Mixing Ratio

Source	% Uncertainty
Forward parameters	5.6
Retrieval method limit	5.3
Instrument calibration	8
Deconvolution of data	4.6
Sum in quadrature	12

Contributions to overall uncertainty in mixing ratio retrievals at peak mixing ratio of lower layer arising from various listed sources.

sunset, and that emission has decreased several fold by sunset and continues its downtrend afterward. Diurnal modeling by *Crutzen et al.* [1992] for photochemical conditions appropriate to McMurdo in 1990 has indicated that only a few percent of midday CIO remains at night in the lower stratosphere. Since this modeling was done to address other issues, we have recently developed a one dimensional photochemical model of our own to specifically analyze the diurnal chemistry of CIO over short periods with careful attention to radiative transfer for large solar zenith angles. We have run it for 1993 stratospheric conditions over McMurdo, with sufficiently short time steps to insure an accurate representation of interspecies and interfamily reactions. An analysis of the diurnal cycle (see paper 2, cited above) indicates that for the conditions of early to mid-September over McMurdo in 1993, the CIO mixing ratio at ~ 20 km would have dropped to $\leq 15\%$ of its midday value by the end of the first 2 hours after stratospheric sunset, and would have averaged about 6% of its midday value during the final 4 hours before dawn that we use for spectral differencing.

Note, however, that a smaller percentage of midday CIO will be converted into the dimer at night when starting from small daytime values (such as we find in October; see below), due to the quadratic dependence of dimer formation on CIO concentration. Hence in cases where we deal with smaller midday mixing ratios, an uncorrected day-night difference will underestimate the midday CIO mixing ratio by a larger percentage than that given above. In addition, the general increase of stratospheric temperature for later dates will produce a small shift toward the monomer in the equilibrium between dimer formation and thermal dissociation. Our model calculations indicate that both effects combined require an upward correction of about 25% to the apparent midday CIO mixing ratio for its peak at ~ 18 km, for values reached by October 6 to 7, in contrast with the much smaller September corrections noted above. (These values assume that the 1994 Jet Propulsion Laboratory recommendations for dimer photodissociation and thermal dissociation rates are essentially correct; see paper 2) We will return to these corrections in section 4.

We deconvolve pressure-broadened line shapes using the Chahine-Twomey technique [*Twomey et al.*, 1977] (see also appendix to present article). Since there is a slight tendency for the weighting functions to impose some bias on the resultant profiles, and a greater tendency for the starting profile to bias the result, we have processed all data with two sets of weighting functions (Figure A1a of the appendix) chosen to maximize at complementing altitudes, and two quite different initial profiles (Figure A1b). The weighting functions are the same as were used in our analysis of 1992 CIO data from McMurdo [*Emmons et al.*, 1995]. We have reduced the number of starting profiles from the four used in that analysis to two after determining that this causes a negligible change in the average of the retrieved profiles. All four permutations of starting profiles and weighting functions were used, and the resulting profiles were averaged to obtain the results shown below. All four profiles from a given spectrum were typically quite close together in the range below 25–30 km. Above that, discrepancies were typically greater, due to the weakness of emission from the higher-altitude layer and the difficulty of extracting an unambiguous upper-layer solution from the data in the presence of a strong, dominating low layer signal. Figure 1 gives a typical result (for September 18 to 20) showing the average and the extreme range covered by the four profiles recovered from the data.

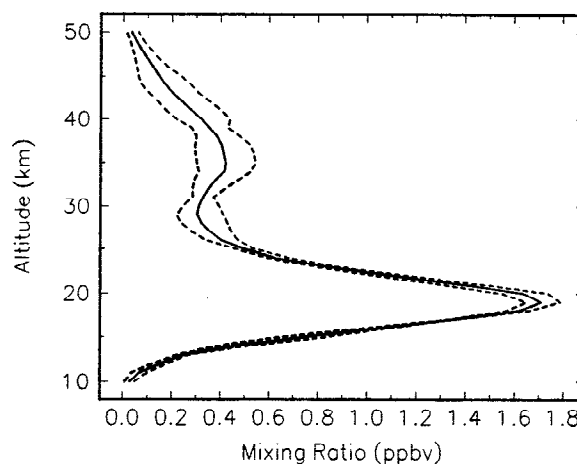


Figure 1. The average (solid line) and envelope of extremes from deconvolutions of the (typical) data for September 18–20, using permutations of the weighting functions and starting profiles in Figure A1 of the appendix. The uncertainties illustrated by the envelope of extremes represent only the "deconvolution" portion of uncertainties in Table 1, as a function of altitude, and not the overall uncertainty.

Below approximately 16 km, the influence of the initializing profiles rapidly comes to dominate the recovered profiles, since the bandwidth limit of 600 MHz causes the weighting functions for lowest altitude (greatest frequency range from line center) to exert little influence on the retrievals below this range. A reasonable lower profile has been established by using an approximation of the ER-2 measurements from within the 1987 Antarctic vortex in the 13 to 16 km range [*Brune et al.*, 1989; corrected by *Anderson et al.*, 1991] in the larger of the two initialization profiles (Figure A1b).

4. Observations

With the exception of a brief interval noted below, McMurdo was located well within the Antarctic vortex, as defined by steepest gradients of potential vorticity on the 475 K potential temperature surface (~ 20 km) during the period covered by our observations (see Figure 4 and the accompanying discussion). A selection of CIO spectra, after removal of ozone as described above, is given in Figure 2 to illustrate the evolution in intensity and line shape that occurred through the observing period.

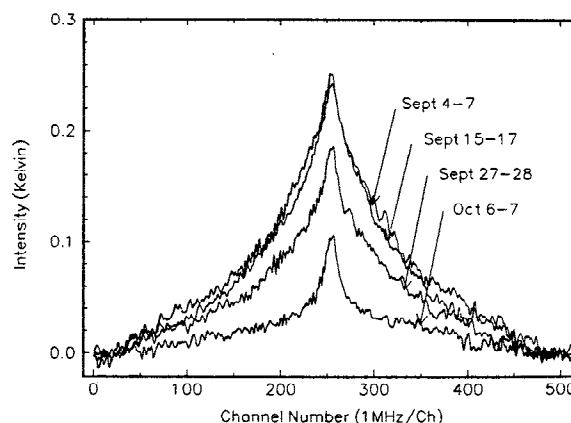


Figure 2. A sample of pressure-broadened CIO spectra after day-minus-night differencing, showing change of intensity and shape with time. Spectra have been grouped into 2- or 3-day sets, as indicated, to increase S/N ratio before deconvolution. Line center frequency (channel 256) is 278.633 GHz.

Very strong emission from CIO in the lower stratosphere was detected on September 4, our first day of regular observations, and continued through most of September. Although this emission intensity was already greater by early September than we have ever measured in previous years during any part of September, line shape deconvolution indicates that the cause was a thicker layer of CIO, extending well into the 20 to 30 km region, while the peak mixing ratio was only mildly greater at the center of the layer. Between September 4 and 23, the layer gradually thinned due to a decreasing mixing ratio in the 23 to 30 km region, the altitude of peak mixing ratio dropped from ~21 to ~18 km, and the maximum mixing ratio varied slightly, from ~1.4 ppbv to ~1.8 ppbv. This history is shown in Figure 3 in the form of a contour map. In this figure, values have not been corrected for the underestimations produced by day-minus-night differencing discussed under section 3. We have chosen here not to make data corrections which are to some extent model dependent, but will, wherever reasonable, indicate in the text how large we believe the corrections to be, and how they affect conclusions drawn from the data.

Table 2 lists the column densities derived from retrieved profiles for each of the day groups used to create Figure 3. The column values have been integrated over the range 15 to 30 km. If extended to 35 km, the column densities are increased by less than 3% for any given entry. The listed uncertainties represent only the spread in values derived from the set of retrieved profiles for each data set, and are listed to show the high internal consistency in fitting the integrated line intensity. The uncertainties listed in Table 1 arising from calibration and "forward" parameters should be included in quadrature, so that the full uncertainty for each entry ranges from ~10% to 11%. Again, we have not corrected entries for the underestimation caused by day-night differencing.

The maximum mixing ratio of ~1.8 ppbv reached on September 21-23 (~1.9 ppbv if corrected for day-night differencing as in section 3) was followed by a very swift decrease, so that the average over September 24-26 was a peak

Table 2. Integrated Column Density, 15-30 km Versus Time

Date	Column Density [10^{15} mol./cm ²]
Sept. 4-7	1.94 ± 0.01
Sept. 11-13	1.94 ± 0.01
Sept. 15-17	2.24 ± 0.01
Sept. 18-20	2.30 ± 0.02
Sept. 21-23	2.35 ± 0.05
Sept. 24-26	0.92 ± 0.05
Sept. 27-28	1.61 ± 0.03
Sept. 30-Oct. 1	2.08 ± 0.08
Oct. 2-3	0.90 ± 0.02
Oct. 6-7	0.62 ± 0.02
Oct. 8-9	0.27 ± 0.01

Values here have not been corrected for possible underestimations due to day-minus-night data processing as discussed in section 4. Uncertainties are based only on the spread of column densities from the four different deconvolutions. See text for discussion of other uncertainties, which sum in quadrature to 10-11%.

mixing ratio of only ~0.6 ppbv (uncorrected) or ~0.75 ppbv corrected. This gradually increased over the next several days to ~1.8 again by September 30 to October 1, then underwent a second rapid and apparently final decline, well under way by October 2-3, with further steady decrease until we stopped observing on October 10.

The sharp decrease and recovery between September 22 and September 30 is clearly the product of a shift in vortex position over McMurdo, as illustrated in Figure 4, where Ertel's potential vorticity contours are plotted for the 475 K potential temperature surface (~20 km). The inner contours move over McMurdo briefly on September 24-25, then retreat northward again. It is interesting to note the rather extreme drop in CIO that occurred near the inner edge of steep potential vorticity gradients (EPV magnitude $\sim 5.2 \cdot 10^{-5}$), indicating that high concentrations of CIO do not extend very far into the vortex boundary region. During

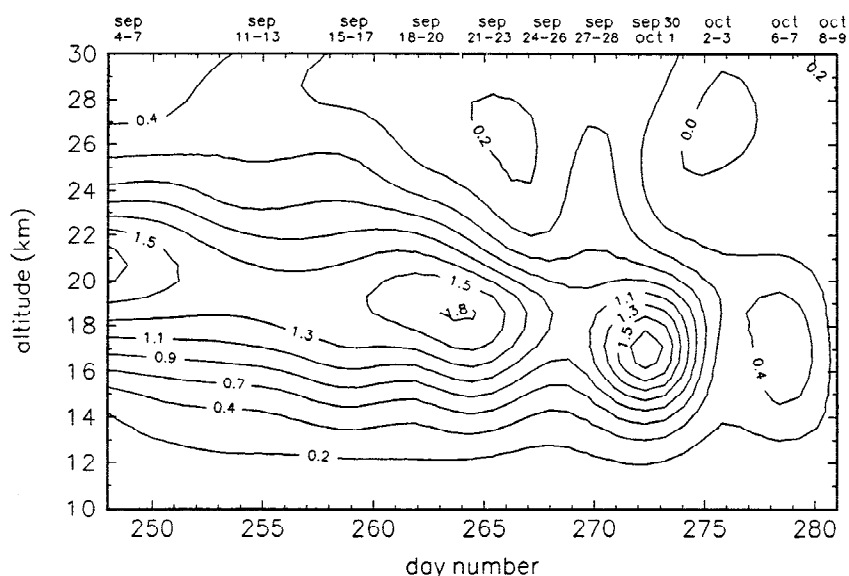
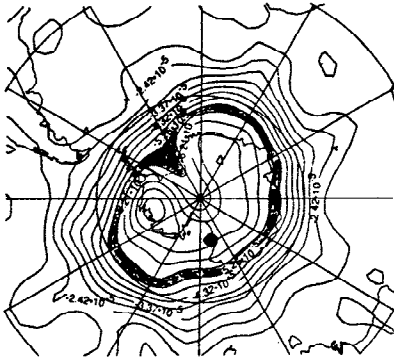
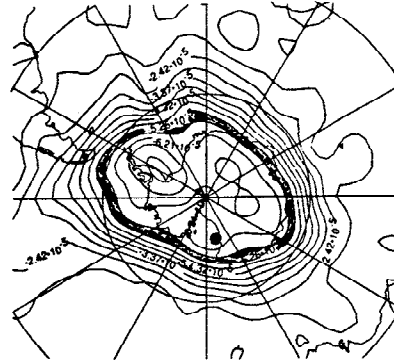
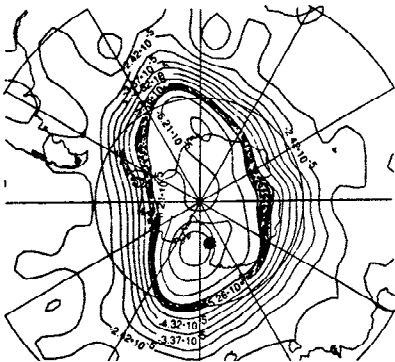
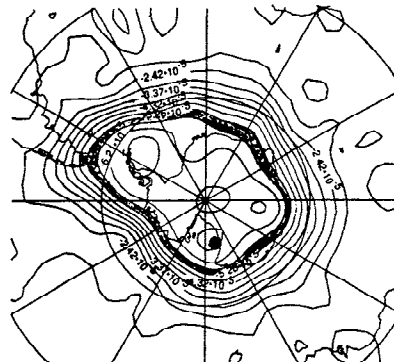
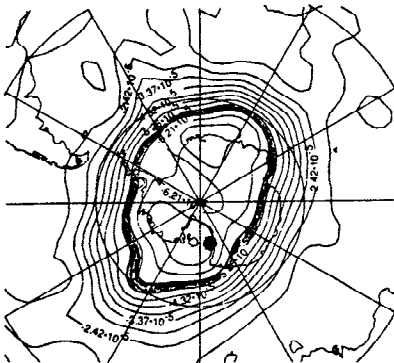
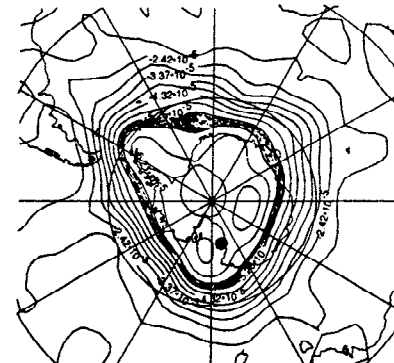
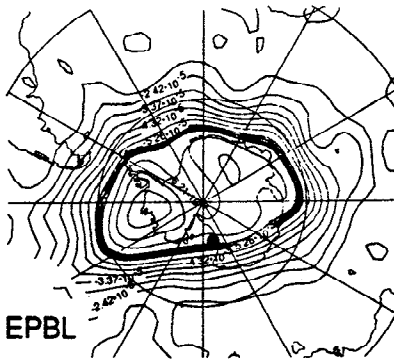
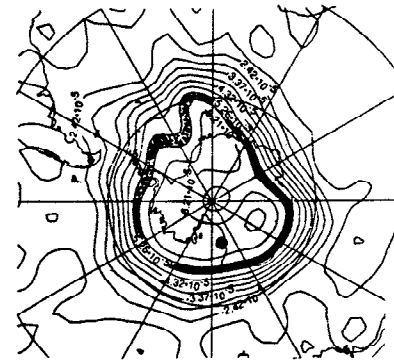


Figure 3. Contour map of CIO profile evolution between 10 and 30 km versus day number. Individual profiles have been retrieved for each of the sets of days listed along the top of the graph. These dates are located at their equivalent day number. The contour values are in parts per billion by volume, and have not been corrected for underestimation of values caused by day-minus-night differencing; see text.

12 UTC on 5 September, 1993 on the 475.0 K surface
Grid: GG5X212 UTC on 26 September, 1993 on the 475.0 K surface
Grid: GG5X212 UTC on 16 September, 1993 on the 475.0 K surface
Grid: GG5X212 UTC on 27 September, 1993 on the 475.0 K surface
Grid: GG5X212 UTC on 21 September, 1993 on the 475.0 K surface
Grid: GG5X212 UTC on 30 September, 1993 on the 475.0 K surface
Grid: GG5X212 UTC on 24 September, 1993 on the 475.0 K surface
Grid: GG5X2

NMC EPBL

12 UTC on 5 October, 1993 on the 475.0 K surface
Grid: GG5X2

GSFC

Figure 4. Ertel's potential vorticity derived from NMC data. The shaded contour lies between -5.2 and $-5.8 \cdot 10^{-5}$ $\text{K} \cdot \text{m}^2/\text{kg} \cdot \text{s}$. McMurdo is marked by the dot a little below center on each map.

the first 10 days of October, the McMurdo region was again well inside the vortex boundary (Figure 4). It thus appears that the rapid "final" decline of low-altitude CIO in early October represented a chemical rather than a meteorological event. It should be noted however that the apparent rapid rate of decline to small values during early October in Figure 3 will be diminished, if an appropriate correction for day-night differencing is applied to the October data, as discussed above.

In paper 2, we have modeled the longer-term evolution of CIO, as well as its diurnal cycle, for conditions appropriate to the 1993 stratosphere over McMurdo. We show that the observed trend of CIO through September and its rapid disappearance in early October may be reproduced in the model by adjusting downward transport, surface loading (for heterogeneous processing), and temperature changes within the error bounds of current measurements. *Crutzen et al.* [1992] have modeled the secular evolution of CIO for the Antarctic vortex conditions of 1990 (specifically considering new chemical pathways for conversion of HCl to active chlorine) and obtained results qualitatively similar to ours, with details dependent on the somewhat different meteorological conditions of 1990, and slightly different assumptions about surface loading and downward transport.

Figure 5 shows 1993 temperatures over McMurdo, derived from National Meteorological Center (NMC) data. We have checked the lowest NMC temperatures (altitude and value) against local measurements from ozonesonde flights at McMurdo by the University of Wyoming (B. Johnson, private communication, 1993) and find quite good agreement ($\pm 1^\circ\text{C}$, ± 1.5 km) for all days when balloons were flown. The vertical range and prolonged period of temperatures of ≤ 195 K is unusual. Both very low temperatures and midwinter PSC formation at unusually high altitudes were detected by lidar probing of air passing over McMurdo during the austral winter (A. Adriani, private communication, 1993), indicating that these conditions had persisted for some time. Despite the continued cold temperatures, very little PSC activity was observed over McMurdo after September 1 (A. Adriani, private communication, 1994), indicating that the early dehydration and denoxification in 1993 was quite thorough.

Figures 4 and 6 show an obvious temporal similarity between the decline in altitude of the peak mixing ratio with time and the

decline in altitude of the lowest stratospheric temperatures. We consider here whether a causal relationship between CIO dimer formation and temperature is serving to create a false impression of declining CIO. Note that the stratosphere at ~ 21 km, for instance, increases in temperature by about 18 K between day 260 and 275. Thermal decomposition of the CIO dimer will shift equilibrium toward the monomer, and the day-night difference in CIO at this altitude would become less, giving the appearance of a drop in midday CIO in our processed data. We have tested this hypothesis using the model described in paper 2, and find that at $T = 188$ K, typical of 21 km in the first half of September, day-night differencing yields about 94% of the true midday CIO, whereas around October 1, with $T = \sim 209$ K, we would see only about 55% of the true midday CIO through day-night differencing; that is, the true mixing ratio at 21 km on about October 1 would be about 1.05 ppb rather than the apparent value of 0.58 indicated in Figure 3. Application of temperature corrections would thus moderate the rate of drop in peak mixing ratio altitude, but not eliminate it. Finally, we note that both recent theoretical studies [e.g., *Manney et al.*, 1994; *Rosenfeld et al.*, 1994] and measurements (S. Crewell, D. Cheng, C. Trimble, and R. L. de Zafra, Millimeter-wave spectroscopic measurements over the South Pole 2: A study of stratospheric dynamics using N_2O observations, submitted to *J. Geophys. Res.*, 1995), show that downward transport in the range of 50 m/day is a persistent feature that continues throughout September (i.e., well after sunrise) in the antarctic vortex.

5. Correlation With Ozone Loss

PSC processing at altitudes higher than usual would have led to the increased active chlorine that we found present (as CIO) in the 20 to 30 km range in early September, and is consistent with the somewhat higher altitudes to which ozone depletion extended in 1993 relative to most previous years [B. J. Johnson, private communication, 1993]. We note that the three-body reaction needed for CIO dimer formation causes a rapid decrease in the efficiency of the dimer-based catalytic cycle with increasing altitude, however (e.g., see paper 2) so that the large amount of CIO is disproportionate to its weaker effect on ozone depletion at, say, 22 to 26 km.

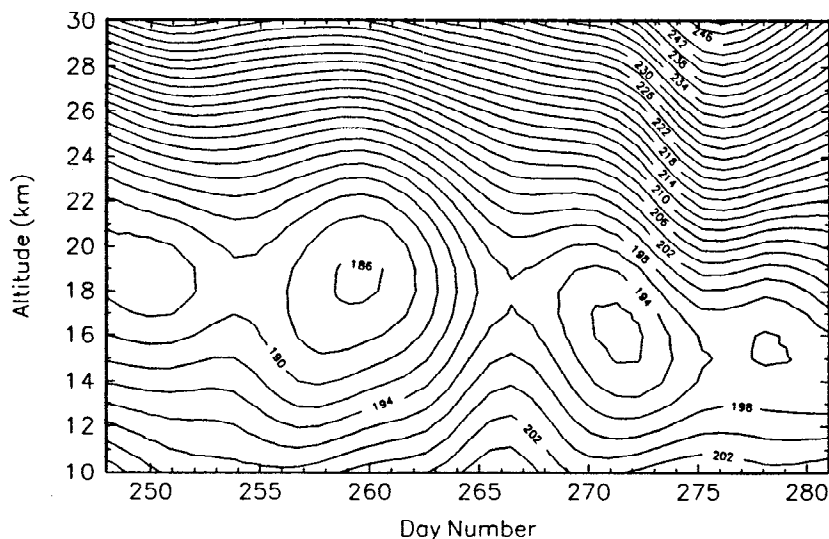


Figure 5. 1993 temperature contours over McMurdo from NMC data, typically at 2-day intervals.

The issue of comparing ozone concentration and loss rates with CIO concentration is complicated by the aforementioned downward transport in the vortex. This will increase ozone concentration at the altitudes being considered, while having a more complex effect on CIO, depending on the prior history of heterogeneous processing. In any case, an increasing mixing ratio of CIO at lower altitudes as time progresses (Figure 3), produces a local acceleration of the ozone loss rate through the pressure dependence of the three-body dimer formation process, as well as through its quadratic dependence on CIO concentration.

Ozone loss rates versus altitude from McMurdo 1993 ozonesonde flights are given by B. J. Johnson et al. [*Geophysical Res. Lett.*, 1994]. In the 22 to 24 km region, they find a moderate O₃ depletion rate, stopping about day 263 to 268 (September 20 to 25), in qualitative agreement with the drop in CIO mixing ratio we note in this same altitude and time period. By day 275 (October 2), ozone depletion has essentially ceased rather quickly at all altitudes, in good agreement with the abrupt decline of CIO noted here. There is no evidence, however, for the acceleration of ozone loss in the 16 to 20 km region during September that would be expected from the arguments given above. We show in paper 2 that downward transport consistent with current estimates [e.g., *Rosenfield et al.* 1994; *Manney et al.*, 1994] will, however, increase the concentration of ozone within the altitude region being considered at a rate just about sufficient to overcome the acceleration in ozone depletion caused by increasing CIO, with the net result of nearly linear ozone depletion versus time.

6. Summary

We have obtained a sustained record of CIO profile measurements over McMurdo Station, Antarctica, during the austral spring of 1993, a year marked by unusually cold temperatures extending to unusually high altitude, strong early PSC formation, lingering low altitude Pinatubo aerosols, and extreme springtime ozone loss. With the exception of a brief interlude in late September, McMurdo was well within the vortex boundary during the period of our observations (September 4 to October 10), and provided a good location for monitoring the long-term evolution of CIO during formation of a major ozone hole event. Our measurements reveal relatively large mixing ratios of CIO in the 20 to 30 km region in early September, which steadily decrease through the month, accompanied by a strong increase in the mixing ratio at ~17 km, with the effect that the peak mixing ratio steadily shifts to lower altitudes, consistent with continued downward transport of stratospheric air through September. We note that a very different impression of the evolution of CIO might be deduced if observations were restricted to ≤ 18 km, characteristic of the altitude limit for ER-2 aircraft sampling. We point out, however, that the decline in altitude of the peak mixing ratio through September is somewhat exaggerated as depicted in Figure 3. This is a consequence of the effect of uncorrected day-minus-night processing as the amounts of CIO diminish above ~20 km, as well as an increase in stratospheric temperatures with time in that region. (See section 4 for an explanation of both these points.) In a companion paper (paper 2), we provide a quantitative model estimate of these corrections. We have chosen not to alter the data given here with these model-derived and model-dependent corrections, but have discussed their range of effect on our data by examples.

A short-term decrease in CIO occurred around September 25, caused by a brief shift of the vortex, followed by a rapid recovery to nearly its earlier values within a few days. A final rapid depletion of lower stratospheric CIO began during the first few days of October when the lower stratosphere over McMurdo was well within the vortex boundary again, apparently marking a rapid chemical deactivation of chlorine. The timing of this coincides very closely with the cessation of ozone depletion determined from University of Wyoming ozonesonde flights over McMurdo. We show in paper 2 that heterogeneous processing by a relatively small surface loading by residual PSCs above 16 km is enough to hold Cl in active forms until the rapid increase in stratospheric temperature at this time destroys all PSCs. Active Cl is then quickly transferred to its inactive reservoirs (HCl and ClONO₂), causing a rapid decline in CIO consistent with that seen in our measurements. Similar results have been obtained by *Crutzen et al.* [1992] in an earlier chemical modeling of the 1990 stratosphere over McMurdo.

Appendix: Profile Accuracy

We give here a brief discussion concerning the accuracy with which vertical profiles may be recovered from pressure-broadened line shapes using the Chahine-Twomey deconvolution method [*Twomey et al.* 1977; Additional discussion and examples may be found in *Emmons and de Zafra* [1994]. This method is an iterative one that begins with an initial vertical profile whose forward-calculated line shape is compared with the spectral data. The profile is altered to produce successively better fits, using a set of frequency-dependent weighting functions to compare and adjust segments of the vertical profile against corresponding segments of the frequency spectrum. The method does not yield a direct error estimate as an output of the deconvolution, and indirect methods must be used to characterize the uncertainties. The sources of error arise (1) from uncertainties in the "forward" calculation of line shape and intensity and (2) from uncertainties in the line shape inversion or deconvolution process, which in principle cannot yield a unique answer, even for a perfect, noise-free spectrum. Moreover, the range of acceptable solutions expands rather rapidly as the rms noise/signal ratio becomes larger than a few percent.

Relatively small uncertainties are involved in the forward calculation. We estimate that uncertainty in the spectral line strength for CIO results in a retrieval uncertainty of $\leq 1\%$, and uncertainty in the pressure broadening coefficient and its temperature dependence over the range 200 to 300 K collectively produce $\leq 3\%$ error [*Oh and Cohen*, 1994; *J. J. Oh and A. E. Cohen*, personal communication, 1994]. Technically, these are systematic errors which would uniformly affect all retrievals for a given line. Since we do not know what sign each may have, we treat them here as random uncertainties to be added in quadrature with other uncertainties in the forward calculation. The remaining forward uncertainties involve the atmospheric temperature and pressure profiles, which would cause a systematic error in a single retrieval, but a random error for retrievals covering several days, assuming no systematic errors in the atmospheric data base being used. Our analysis shows that a uniform 5% error in pressure at all altitudes would lead to a 1% error in retrieved vertical profile for CIO, and a similar 5°C error in temperature would cause a 4.5% error in retrieval. All uncertainties, added in quadrature, give an overall

forward uncertainty of 5.6% in retrieved mixing ratio at both 18 km and 37 km altitude, and an uncertainty of ~ 1 km in the altitude at which the peak mixing ratios occur for separate layers near these altitudes.

We have estimated separate components of uncertainty in the line shape inversion process as follows: (1) There is an inherent uncertainty in finding a solution by inversion stemming from the non-uniqueness of the process. To characterize this, a "true" vertical profile is assumed which is close to that for ClO in the Antarctic stratosphere. A pressure-broadened noise-free line shape is synthesized for this distribution by forward calculation, and deconvolved using all permutations of the weighting functions and initial profiles shown in Figure A1. Deviation of the average of the resulting profiles in this noise-free case from the true profile is given as the "retrieval method limit" uncertainty in Table 1. (2) To estimate the uncertainty produced by noise in the real spectra, our actual data are deconvolved using all permutations of the weighting functions and initial profiles. The deviation of this set of results from their own average is then computed as a function of altitude. The value at the peak of the lower layer is listed as the "spectral noise" contribution in Table 1, and typical results as a function of altitude are shown in Figure 1.

Instrument calibration consists of determining the sensitivity of the receiver to incoming radiation, and determining the exact pointing elevation of the instrument against the sky in order to correct actual atmospheric path lengths to a standard zenith direction. The methods involved are described in detail by Parrish *et al.* [1988] and de Zafra [1995]. The present level of uncertainty in overall calibration is estimated to be 8%. Finally, we assume that the different sources of error may be added in quadrature to obtain the overall value given in Table 1.

Acknowledgments. This research was supported by grants NAGW-2182 and NAG-11354 from NASA's Upper Atmospheric Research Program and UARS Correlative Research Program, respectively, and by NSF grant DPP9117159. We also express thanks to L. L. Lait, P. A. Newman, and M. R. Schoeberl for use of NASA's GSFC "AutoMailer" system from which we obtained the potential vorticity plots of Figure 4, and to the many employees of Antarctic Support

Associates, Inc., who strive with some success to make our Antarctic field work closer to pleasure than pain.

References

- Anderson, J. G., D. W. Toohey, and W. H. Brune, Free radicals within the Antarctic vortex: The role of CFCs in Antarctic ozone loss, *Science*, **251**, 39-46, 1991.
- Brune, W. H., J. G. Anderson, and K. R. Chan, In situ observations of ClO in the Antarctic: ER-2 aircraft results from 54°S to 72°S latitude, *J. Geophys. Res.*, **94**, 16,649-16,664, 1989.
- Crutzen, P. J., R. Mueller, C. Bruehl, and T. Peter, On the potential importance of the gas phase reaction $\text{CH}_3\text{O}_2 + \text{ClO} \rightarrow \text{ClOO} + \text{CH}_3\text{O}$ and the heterogeneous reaction $\text{HOCl} + \text{HCl} \rightarrow \text{H}_2\text{O} + \text{Cl}_2$ in "ozone hole" chemistry, *Geophys. Res. Lett.*, **19**, 1113-1116, 1992.
- de Zafra, R. L. The ground-based measurement of stratospheric trace gases using quantitative millimeter wave emission spectroscopy, in *Proceedings of the International School of Physics "Enrico Fermi"*, Course CXXIV, Diagnostic Tools in Atmospheric Physics, (in press, 1995).
- de Zafra, R. L., M. Jaramillo, A. Parrish, P. M. Solomon, B. Connor, and J. W. Barrett, High concentrations of chlorine monoxide at low altitudes in the antarctic spring stratosphere: Diurnal variation, *Nature*, **328**, 408-411, 1987.
- de Zafra, R. L., M. Jaramillo, J. W. Barrett, L. K. Emmons, P. M. Solomon, and A. Parrish, New observations of a large concentration of ClO in the springtime lower stratosphere over Antarctica and its implications for ozone-depleting chemistry, *J. Geophys. Res.*, **94**, 11,423-11,428, 1989.
- de Zafra, R. L., W. H. Mallison, M. Jaramillo, J. M. Reeves, L. K. Emmons, and D. T. Shindell, A new high-sensitivity superconducting receiver for mm-wave remote spectroscopy of the stratosphere, *Proceedings of the 1992 Quadrennial Ozone Symposium*, Charlottesville, Va., (NASA Conference Publ. 3266), 719-722, 1994.
- Emmons, L. K., and R. L. de Zafra, Accuracy of profile retrievals from mm-wave spectra of ClO and N_2O , in *International Geosciences and Remote Sensing Symposium Proceedings: IGARSS '94*, Rep. 94CH3378-7, vol. III, pp. 1684-1686, Inst. of Electr. and Electron. Eng., Piscataway, N. J., 1994.
- Emmons, L. K., D. T. Shindell, J. M. Reeves, and R. L. de Zafra, Stratospheric ClO profiles from McMurdo Station, Antarctica, spring 1992, *J. Geophys. Res.*, **100**, 3049-3055, 1995.
- Hofmann, D. J., S. J. Oltmans, J. A. Lathrop, J. M. Harris, and H. Voemel, Record low ozone at the South Pole in the spring of 1993, *Geophys. Res. Lett.*, **21**, 421-424, 1994.
- Manney, G. L., R. W. Zurek, A. O'Neill, and R. Swinbank, On the motion of air through the stratospheric polar vortex, *J. Atmos. Sci.*, **51**, 2957-2972, 1994.
- Oh, J. J., and A. E. Cohen, Pressure broadening of ClO by N_2 and O_2 near 204 and 649 GHz, and new frequency measurements between 632 and 725 GHz, *J. Quant. Spectrosc. and Radiat. Transfer.*, **52**, 151-156, 1994.
- Parrish, A., R. L. de Zafra, P. M. Solomon, and J. W. Barrett, A ground-based technique for millimeter wave spectroscopic observations of stratospheric trace constituents, *Radio Sci.*, **23**, 106-118, 1988.
- Rosenfield, J. E., P. A. Newman, and M. R. Schoeberl, Computations of diabatic descent in the stratospheric polar vortex, *J. Geophys. Res.*, **99**, 16,677-16,689, 1994.
- Solomon, P. M., B. Connor, R. L. de Zafra, A. Parrish, J. W. Barrett, and M. Jaramillo, High concentrations of chlorine monoxide at low altitudes in the antarctic spring stratosphere: Secular variation, *Nature*, **328**, 411-413, 1987.
- Solomon, S., Progress towards a quantitative understanding of Antarctic ozone depletion, *Nature*, **347**, 347-354, 1990.
- Twomey, S., B. Herman, and R. Rabinoﬀ, An extension of the Chahine method of inverting the radiative transfer equation, *J. Atmos. Sci.*, **34**, 1085-1090, 1977.

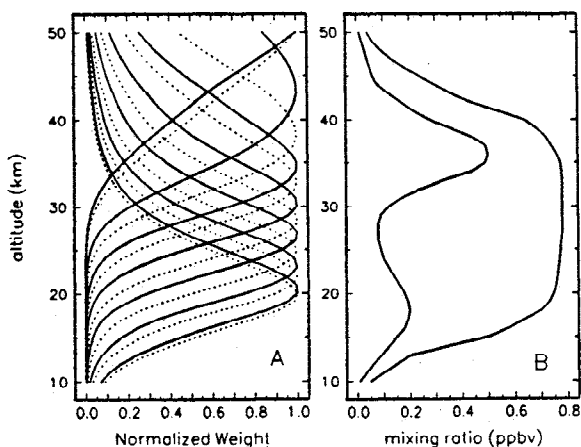


Figure A1. (a) The two sets of weighting functions (solid and dashed) used for the Chahine-Twomey deconvolution of pressure-broadened spectra. (b) The two starting profiles used for deconvolutions. Each retrieved profile is an average of deconvolutions employing the four permutations of these weighting functions and starting profiles.

Waters, J. W., L. Froideveaux, G. L. Manney, W. G. Read, and L. S. Elson, MLS observations of lower stratospheric ClO and O₃ in the 1992 southern hemisphere winter, *Geophys. Res. Lett.*, 20, 1219-1221, 1993.

J. M. Reeves, Department of Atmospheric, Oceanic, and Space Sciences, University of Michigan, Ann Arbor, MI 48109.

R. L. de Zafra and D. T. Shindell, Physics Department, State University of New York, Stony Brook, N.Y. 11794. (email: rdezafra@ccmail.sunysb.edu)

(Received August 24, 1994; revised January 13, 1995; accepted January 13, 1995.)